CFD Airfoil Analysis with High Aspect Ratio in Unmanned Aerial Vehicles

Byung Ryoun Kim, Chakun Cheong, Kyoungwoo Park, and [+]Byeong Sam Kim

***Abstract*—**Shape optimization of the airfoil with high aspect ratio of long endurance unmanned aerial vehicle (UAV) is performed by the multi-objective optimization technology coupled with computational fluid dynamics (CFD). For predicting the aerodynamic characteristics around the airfoil the high-fidelity Navier-Stokes solver is employed and SMOGA (Simple Multi-Objective Genetic Algorithm), which is developed by authors, is used for solving the multi-objective optimization problem. To obtain the optimal solutions of the design variable (i.e., sectional airfoil profile, wing taper ratio and sweep) for high performance of UAVs, both the lift and lift-to-drag ratio are maximized whereas the pitching moment should be minimized, simultaneously. It is found that the lift force and lift-to-drag ratio are linearly dependent and a unique and dominant solution are existed. However, a trade-off phenomenon is observed between the lift-to-drag ratio and pitching moment. As the result of optimization, sixty-five (65) non-dominated Pareto individuals at the cutting edge of design spaces that are decided by airfoil shapes can be obtained.

Keywords— Unmanned aerial vehicle (UAV), Airfoil, CFD, Shape optimization, Lift-to-drag ratio, Genetic Algorithm.

I. Introduction

The UAVs are manufactured for various sizes from the hand-held Micro-Air Vehicle (MAV) [1] to the large-scaled UAV such as Global Hawk, Predator [2] and Theseus Helios and Strato 2C[3]. From the 1980s, the large-scaled UAVs have been developed and proved for their values of security, communication and battle management. Goraj [4] provided the overview of the design activity of civil HALE (high altitude long endurance) UAV (PW114) and reported that the cost of operation could be reduced by improvement of aerodynamic efficiency and optimization of aircraft structures. He redesigned the previous model (PW111) and developed a new airfoil shape with high aspect ratio via aerodynamics analyses for decreasing the load and increasing the lift force. For MALE (medium altitude long endurance) UAVs, Goetzendrof-Grabowski et al.[5] studied on the aerodynamic characteristics to achieve the required aircraft performances. Their work was mainly focused on the reliability and redundancy issues and the high aspect ratio of airfoil was proposed to increase the lift-to-drag ratio. To avoid the conversing to the local optima and to reduce the number of design variables, Painchaud-Ouellet et al. [6] assessed the suitability of non-uniform rational B-splines (NURBS) for the aerodynamic design optimization for various Mach numbers. Pines and Bohorquez [7] suggested that the MAV for urban missions is at least an order of magnitude smaller in length and two orders of magnitude lighter in weight than previously developed aircraft. They also showed that the maximum dimension is less than 15.24cm and the target gross take off weights (GTOW) is up to 100g. Ng and Leng[8] performed the conceptual design of the flying- wing-type MAV with six-design variables including a winglet taper ratio. They employed a genetic algorithm (GA) which uses a real value instead of binary for searching the global optimum. They insisted that the genetic algorithm is more efficient than a conventional SQP-based non-linear optimization problem.

In order to improve the aerodynamic performance of UAVs, designers have to consider many design factors. That is, the airfoil profile, aspect ratio of airfoil and wing taper ratio which are to be the critical design factors to obtain aerodynamically efficient, reliable and stable UAVs are considered as design variables simultaneously. Designer's perceptions, however, are too complicate to understand multi-dimensional design spaces completely.

In the present work, the best airfoil platform shapes of the long endurance UAVs for a high performance are obtained by the multi-objective optimization technique. SMOGA based on GA with multi-objective optimization technique can explore the multi-dimensional design space and find Pareto optima at the frontier of the space. The sectional airfoil profile for the design variables is parameterized with four-Bezier curves. For a three-dimensional wing configuration, two design variables such as a taper ratio and

[+]Byeong Sam Kim was with Hoseo University, Asan city, Korea,. He is now with the School of Mechanical Engineering (corresponding author to provide phone:+82 41 540 5814; fax:82 41 540 5818, e-mail:kbs@hoseo.edu)

Byung Ryoun Kim is PhD candidate with the School of Mechanical Engineering at Hoseo University

Chakun Cheong is with the Mechanical Engineering Department, Hoseo University, Asan, 336-795, Korea (cheong@hoseo.edu).

Kyeonwooi Park is with the Mechanical Engineering Department, Hoseo University, Asan, 336-795, Korea (e-mail:kpark@hoseo.edu).

sweep should be added to the design variable. The lift coefficient, lift-to-drag ratio and pitching moment coefficient are adopted as the objective functions. It is difficult to find Pareto optima in three or more design spaces with typical gradient-based optimizers or weighting objective functions because the design space to explore is dramatically increased. Therefore, in order to obtain the optimal solutions of the design variables, the SMOGA which can include all possible designs in multi-dimensional objective space should be used and it is combined with a reliable solver for Navier-Stokes equation to compute the objective functions accurately. Because the trade-offs among the objective functions can be taken place for a multi-objective optimization or vector-optimization problem, Pareto optima instead of single unique solution are generally existed and they lead to the Pareto frontier in a multi- objective design space.

I. Multi-Objective Optimization

A. Genetic Algorithm

GAs are originated from Fraser's work [9] on the simulation of genetic systems, Holland's study [10] on adaptation in natural and artificial systems and Goldberg's development [11] on various applications and multi-objectives. The GA mimics evolutionary characteristics of nature works with artificial populations which are collections of the searching elements in the entire design space. It is a unique global optimum algorithm based on the mechanism of reproductions and mutations [11]-[12]. The creatures in the nature have adjusted themselves to their circumstance even though it has dynamically changed every moment. The well-fitted individuals can only survive and have more chances to mate with the others and finally to get the similar and superior offspring.

B. Genetic Operations

New individuals for the next generation can be obtained by genetic operations such as selection, crossover, and mutation. The selection is a series of processes to choose a parent for the next generation and also provides a guide of evolutions. For the multi-objectives like this study, the tournament selection is generally used instead of a general roulette wheel. Pairs of candidates are randomly picked from the population. An individual with higher fitness or a non-dominated Pareto individual is copied into the mating pool. The competitions are performed for the number of tournament (n) and these can manage the selection pressure. The high selection pressure may find the local optima although it leads to a fast convergence because of insufficient exploration of the design space. Pareto domination is defined as follows;

$$\bar{x} \underset{p}{>} \bar{y} \Leftrightarrow \left(\forall i F_i(\bar{x}) \geq F_i(\bar{y})\right) \cap \left(\exists j F_j(\bar{x}) \geq F_j(\bar{y})\right) \quad (1)$$

where $\bar{x}$, $\bar{y}$, F_i and F_j represent the vector values of individual x and y . Subscripts i and j are i-th and j-th objective function, respectively.

The number of crossover points is closely related to the survival of schema that is the meaningful pattern in the gene. Short and/or low-fit schema becomes a longer and higher one as the evolution is proceeded. Booker [13] suggested that the two-point crossover is favorable for the schema's survival. Therefore, it is used and a single-point crossover is also adopted as an option in the present work. Since the selection and crossover are deterministically progressed, it is difficult to generate new genes completely in order to extend the searching area. The deficiency of searching design space can lead to the local optima solution. The mutation helps to keep the balance between the exploration and exploitation to find the global optima. In the present work, a new individual that has a genetic twin in the new generation is ignored for keeping the diversity of the population. The properties of adjacent individuals in the design space are similar to each other. It is necessary to control the number of individual within the radius of niche for extending the exploration. The existence of local optima is very attractive at the early stage of evolution. The offspring tends to come together around the local optimum points instead of global ones, which leads early mature convergence. The niche is able to control the exploration of the design space and prevent a GA from early mature convergence. In the present work, the binary distance between two individuals instead of the n dimensional norm is adopted which is defined as the following equation;

$$\frac{r_{ij}}{R} = \sum_{k=1}^{L} \left[\frac{\left| d_i - d_j \right|}{R} \right]_k = \sum_{k=1}^{L} \left[\frac{m \cdot \Delta x}{n \cdot \Delta x} \right]_k = \sum_{k=1}^{L} \left[\frac{m}{n} \right]_k \quad (2)$$

where $\left| d_i - d_j \right|$ is the distance between i and j individuals in k variable, m is the binary distance, and n is the niche binary distance. The niche radius in the real design space cannot represent all niches at once and therefore the niche radii for each design variable are required. In the case of binary distance, however, only one niche radius is sufficient.

II. Shape of Airfoil

There are many ways to represent the airfoil profile: combination of a few basic airfoils, using a spline curves and Bezier curves. Among them, it is well known that the Bezier curves with a few number of control points can reproduce various airfoils easily and precisely.

Fig. 1 shows the schematic diagram of airfoil using the

Bezier curves. The airfoil is parameterized with four Bezier curves: 4th-order Bezier curves for the leading edge and 3rd-order for the trailing edge. As shown in Fig. 1(a), the airfoil is consisted of six-control points on each side. Except for some continuous or fixed points (i.e., maximum thickness, smooth leading and trailing edges), the number of the design variables are to be eighteen (18). The selection of same coordinate for three control points at the maximum thickness can guarantee that continuity c_0 and c_1 are satisfied so that the design variables for an airfoil can be reduced by eleven (11) [14]. Lee et al. insisted that the reduced design variables (i.e., from 18 to 11) can obtain by performing the correlation analyses for the design variables, objective functions and deviation of the design variables. Especially, for three-dimensional airfoil specification, the taper ratio (CR) and sweep (ω) should be added as the design variables as shown in Fig. 1(b). Thus, in this study, the number of design variables becomes thirteen (13).

The baseline geometry of airfoil is placed along the trailing edge and the chord at the tip shrinks according to the taper ratio.

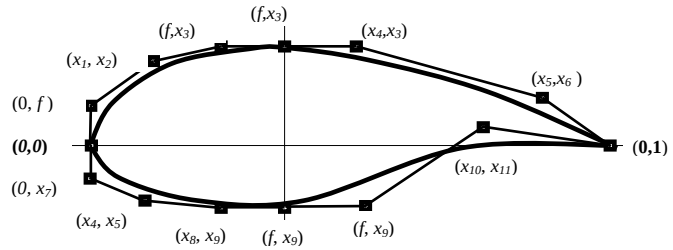

(a) Cross-sectional wing shape and design variables

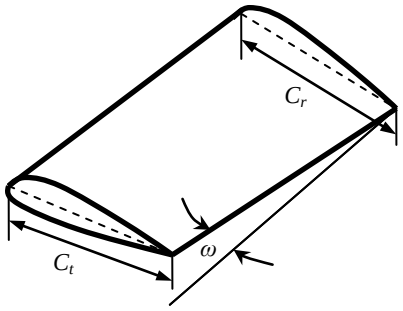

(b) Taper ratio (CR = C_t / C_r) and sweep (ω)

Fig. 1 Three-dimensional wing specification for optimization

The sweep of zero ($\omega = 0$) means that two trailing edges both at the root and tip are located side by side at $CR = 1$. On the other hand, when the value of sweep is a positive one (+), the wing sweep goes forward. In this work, the half span is considered as a computational domain due to the symmetrical configuration of airfoil.

I. Results and Discussion

The SMOGA based on GA which was developed by the authors is adopted for the optimization of UAV airfoil. This can handle the intricate multi-objective optimization problems without both the weighting factors and normalizations. The target of this work is to obtain the three-dimensional optimal shape of the UAV airfoils. For this, the SMOGA is integrated to the CFD analyzer [15] which can predict the aerodynamic characteristics accurately. It is assumed that the fluid is incompressible and the flow is steady-state and turbulent.

In the multi-objective optimization problem, the optimal solutions are classified as the dominated and non-dominated ones. The latter is called as the Pareto optima which are placed along the front line of the multi-dimensional design space and they can be obtained by the SMOGA. Before the direct evaluation is performed, the values of objective functions for the new individual are searched in the running pool where the calculated values are already saved in the previous iterative step. If the same design is not found, the computational analysis is performed by the CFD analyzer that independently executes a series of jobs: grid generation, flow analysis, evaluation of the results, and creation of files including the value of objective function. The first generation is randomly generated and then the offspring are created by the genetic operations such as selection, crossover and mutation.

A. Formulation of Optimization Problem

The optimization problem considered in this study can be expressed mathematically and it is written as,

$$\text{Find} \quad \boldsymbol{X} = \{X_1, X_2, \cdots X_m\}^T \tag{3}$$

$$\text{to maximize } \boldsymbol{F}_1(\boldsymbol{X}) = \boldsymbol{C_L} \tag{4}$$

$$\text{to maximize } \boldsymbol{F}_2(\boldsymbol{X}) = \boldsymbol{C_L} / \boldsymbol{C_D} \tag{5}$$

$$\text{to minimize } \boldsymbol{F}_3(\boldsymbol{X}) = \boldsymbol{C_{M,1/4}} \tag{6}$$

$$\text{subjected to} \quad \boldsymbol{X}_i^L \le \boldsymbol{X}_i \le \boldsymbol{X}_i^U \text{ for } i = 1 \sim 13. \tag{7}$$

The lift (C_L), lift-to-drag ratio (C_L / C_D) and pitching moment about a quarter chord ($C_{M,1/4}$) are the objective functions. There are no explicit constraints except for the upper and lower bounds of the design variables ($\boldsymbol{X}_i^L, \boldsymbol{X}_i^U$) as shown in Eq. (7). The optimization is carried out under the normal cruise state such as $\alpha = 2$ (angle of attack), AR = 17.5 and Re = 2.8×10^6.

Table I represents the optimization parameters and the upper and lower bounds of the design variables are listed in Table II. Two cutting lines are used to maximize the life of schema effectively. The dimensions of a design space, which

consists of the number of design variables and resolutions of each design variable, are the most important factors for the optimization. The dimension of a design space is exponentially increased as the number of design variables is linearly increased. The last two design variable (x_{12} and x_{13}) in Table II represents the taper ratio and sweep, respectively.

B. Validation of CFD Model

To validate the accuracy of present CFD model and to check the grid dependency, numerical analysis for the pressure

TABLE I
PARAMETERS FOR GENETIC ALGORITHM

	Values
Population	30
Generation	25
Cross over rate	0.8
Mutation rate	0.5%
Tournament level	2
Niche binary radius	1

TABLE II
UPPER AND LOWER LIMITS OF DESIGN VARIABLES

$\mathbf{X}_i$	$\mathbf{X}_i^L$	$\mathbf{X}_i^U$	$\mathbf{X}_i$	$\mathbf{X}_i^L$	$\mathbf{X}_i^U$
x_1	0.040	0.060	x_8	0.190	0.260
x_2	0.100	0.150	x_9	-0.057	-0.053
x_3	0.055	0.065	x_{10}	-0.030	-0.010
x_4	0.550	0.600	x_{11}	0.730	0.750
x_5	0.010	0.030	x_{12}	0.500	1.000
x_6	0.700	0.950	x_{13}	0.000	3.500
x_7	-0.030	-0.025			

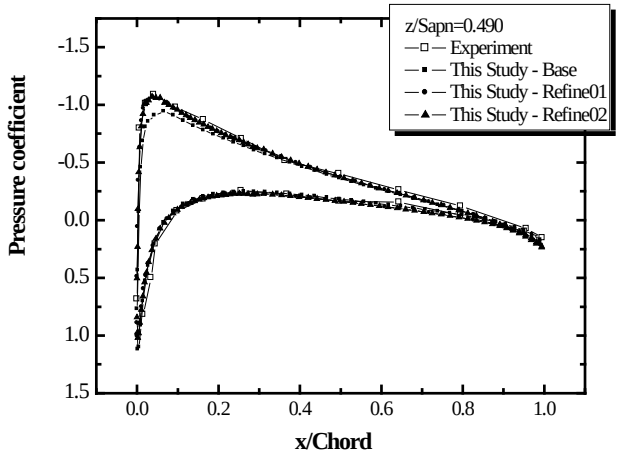

Fig. 2 Pressure distributions of this model and experiments for various grid systems at z/span = 0.49

distribution of an un-tapered rectangular shape of airfoil(*CR*=1) is carried out. The results are also compared with those of experimental ones that were conducted by McAlister and Takahashi [16] for the NACA 0015 with the aspect ratio (AR) of 6.6 and Reynolds number of 2.8×10^6. Fig. 2 presents the pressure distribution (C_p) for various grid systems (i.e., base, refine#1 and refine#2, corresponding to the number of meshes are 220,000, 290,000 and 790,000). The numerical analysis shows a good agreement with the experiment data at except for near the tip. The RNG k-ε turbulence model was used and the near-wall flow was computed using wall functions. To test the grid dependency, the $y^+_{\max}$ values are calculated for three grid systems. For the finest grid, the number of the grid is dramatically increased to match the distributions in the whole domain. According to the pressure distribution and the computational cost, the refine#01 grid (total number of grid is 290,000) is used for the optimization.

C. Optimization

Fig. 3 shows the convergence history for the sweep (w) and taper ratio (*CR*), which are the design variables for three-dimensional airfoil, according to the individual numbers. It can be seen in Fig. 3 that they spread between the lower and upper bounds at early stages and become to converge after 7th- or 8th- evolutions. Finally, the sweep is approached to its lower bound ($\omega \to 0$ degree*)* while the taper ratio is close to its upper bound. This means that the optimized airfoil shape for Pareto optima has a rectangular wing, that is, the sweep of about zero ($\omega \sim 0$) and taper ratio of about unit (*CR*=1). This phenomenon is resulted from the following reasons: because the only aerodynamic forces exerted on the wing surface and the pitching moment at a quarter-chord axis are considered in the present work. The pitching moment is increased as the sweep is increased because the distances between the exerted forces are also increased. Thus, the un-sweep with rectangular wing shape can be a potential candidate of the optimal design. However, it is known that the structure of the wing with a taper ratio is more

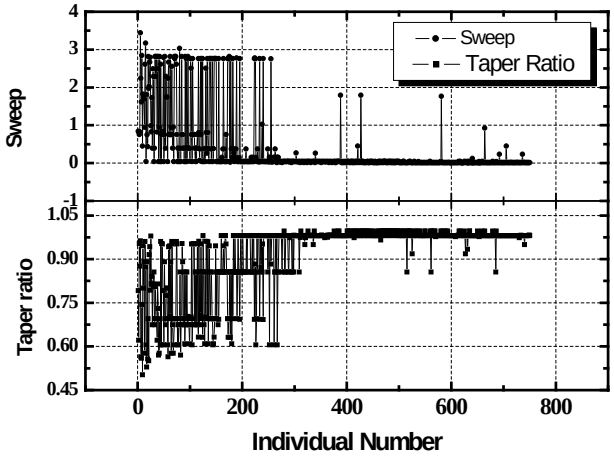

Fig. 3 Convergence history of the taper ratio (CR) and sweep (ω) according to the individual numbers

stable than that of the rectangular wing. This result can be easily validated from the previous applications such as Predator, Helios and Global Hawk. That is, the straight (un-sweep) and tapered wing shape can be the optimized one in real-world long endurance UAVs.

The objective functions can be plotted in three-dimensional space and then Pareto optima are shown in Fig. 4(a). For easy explanation, they can be presented in two-dimensional space so that all individuals in three-dimensional figure are break down to two-dimensional graphs and all individuals are also projected to each direction as shown in Fig. 4(b)-(d). The relations between the lift (C_L) and lift-to-drag ratio (C_L / C_D), which are maximized to obtain the optimal wing shape are presented in Fig. 4(b). Fig. 4(b) shows that the lift-to-drag ratio is increased with the lift because they have to be maximized for the optimization as we expected. All Pareto optima are increased monotonically and Pareto#06 becomes a unique solution and it dominates all the individuals including Pareto optima in this projected design space (lift and lift-to-drag ratio). It is concluded that the relation of lift and lift-to-drag ratio is linearly dependent. However, both the lift to pitching moment and lift-to-drag to pitching moment show the trade-off phenomena as the results of optimization. Fig. 4(c) presents the pitching moment according to the lift. When we only consider them as the objective function, the figure shows that the Pareto optima are located at the lower-right space because the lift is maximized while the pitching moment is minimized. Non-dominated Pareto optima are placed along the frontier lines on the edge of design spaces. Numbered individuals from Pareto optima are arbitrarily selected among the Pareto frontier. The Pareto#01 and Pareto#06 in Fig. 4(c) indicate that they have the lowest pitching moment and the largest lift, respectively. It is also found that the objective function for base model can be observed away from the frontier line and is located at the middle of the dominated individuals as shown in Fig. 4(c) and (d).

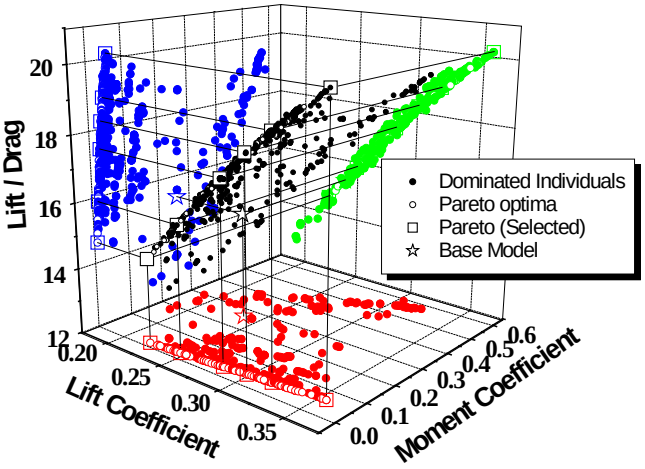

(a) Three-dimensional view for optimization results

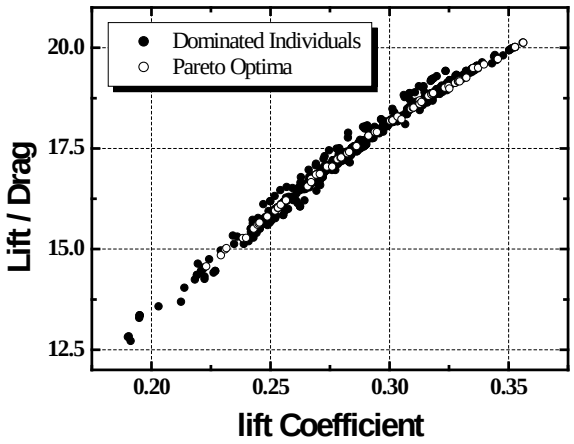

(b) Lift vs. lift-to-drag coefficients for Pareto optima and dominated solutions

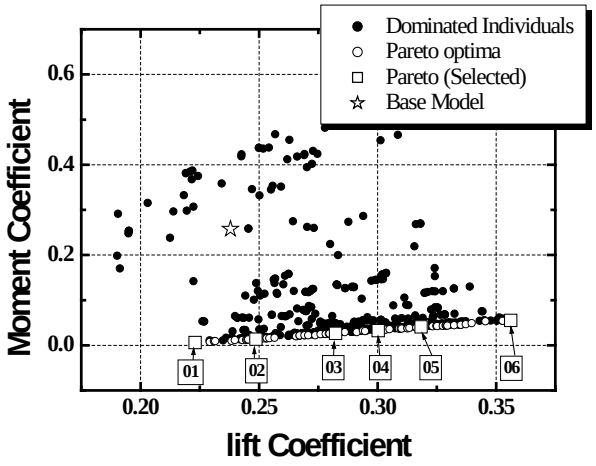

(c) Lift vs. pitching moment for Pareto optima and dominated solutions

Fig. 5 shows the pressure distributions on the wing surface

according to the non-dimensional chord (*x*/*chord*) at the root for three selected Pareto optima (#01, #03 and #6). The corresponding airfoil profiles are also shown at the lower part o f

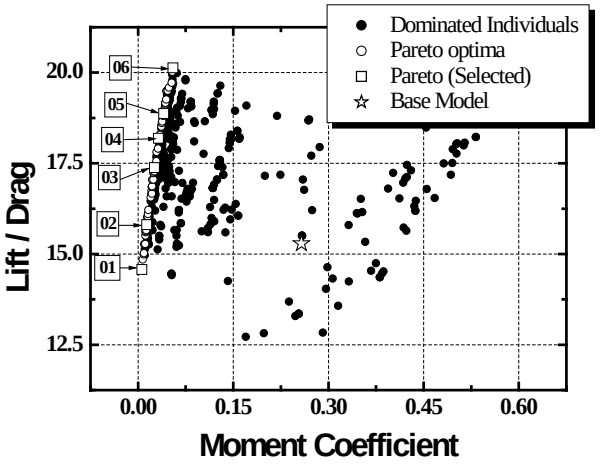

(d) Pitching moment vs. lift-to-drag for Pareto optima and dominated solutions

Fig. 4 Comparison of objective functions

the figure. Note that in this case, sectional airfoil profile becomes a significant factor for the optimization because it determines sectional pressure distributions and forces around the airfoil. It can be seen in the figure that for all Pareto optima the phenomenon of flow separation is not occurred at the location of maximum thickness (*x*/*chord*=0.3) because the optimization is carried out for the case of low angle of attack ($\alpha = 2^o$). In addition, the pressure differences among the Pareto optima are apparently appeared near the trailing edge. This fact leads that a higher pitching moment which is resulted from a larger force is occurred at the trailing edge as the Pareto number is increased. It is also found in the figure that the wing configurations are varied due to the different lift and drag forces as the results of optimization. As shown in the lower box of Fig. 5, the configuration for Pareto#06 is thicker than others and this feature is kept to the trailing edge of wing. The wing shape for Pareto#01, however, is relatively thin and seems to be approximately symmetric airfoil because of the lower value of lift and the smallest pitching moment compared to other Pareto optima. Since the fuselage is excluded for the aerodynamic analysis, the profile and induced drags can only affect a total drag.

The half of profile drag is a friction one resulting from shear stress on the wetted wing surface. However, the variation of the wetted surface area is not severely changed according to the variation of the wing profile. As a result, the friction drag among the listed Pareto optima has only small differences. It is clear that the pressure drag by wing profile and the induced drag by wing arrangement are important to obtain optimized wings.

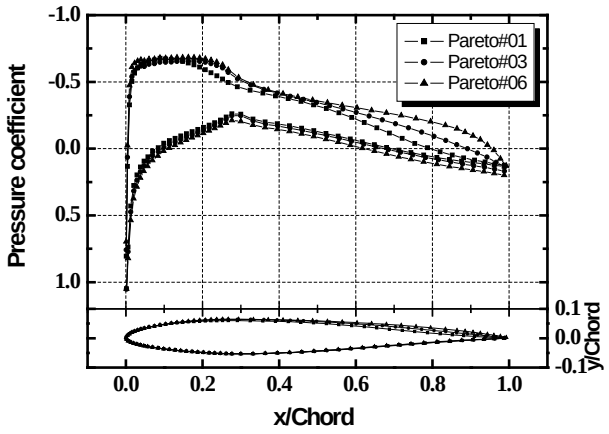

Fig. 5 Pressure distributions and cross-sectional wing shapes at the root for selected Pareto optima

The endurance is one of the keys to achieve the high performance of UAVs. The endurance means the amount of time that the UAV can stay in the air on one load of fuel. For the propeller-driven airplane, Anderson [18] showed the correlation of endurance (*E*) and approximated it as a function of the lift and drag coefficients. The endurance which was proposed by Anderson can be expressed as follows;

$$E = \frac{\eta_{pr}}{c}\sqrt{2\rho_\infty S}\,\frac{C_L^{3/2}}{C_D}\left(W_1^{-1/2} - W_0^{-1/2}\right) \sim \frac{C_L^{3/2}}{C_D} \tag{8}$$

where η_{pr} , c , ρ_∞ , S , W_1 , and W_0 are the propeller efficiency, specific fuel consumption, density, wing area, gross weight of the airplane including everything and weight of the airplane when the fuel tanks are empty, respectively. Especially, $C_L^{3/2}/C_D$ indicates the endurance parameter in Eq. (8) and it can be obtained when the optimization is completed. Figure 6 presents the endurance as a function of angle of attack (α) for the three selected Pareto optima. For all ranges of α , Pareto#06 has the largest value of *E* compare with other Pareto optima because it also has the largest lift-to-drag. It is also found that the maximum value of endurance is occurred at $\alpha = 4^o$ for Pareto#06 and its value is about 24. The interesting fact is also seen in Fig. 6 that the endurances for all Pareto optima have the same value at the angle of attack of 8 degree. It is deduced that increasing in the drag is more rapidly occurred than that of the lift from $\alpha = 4^o$ to $\alpha = 8^o$.

In order to explain the results of shape optimization, the pressure contours around the wing and the optimal shapes of

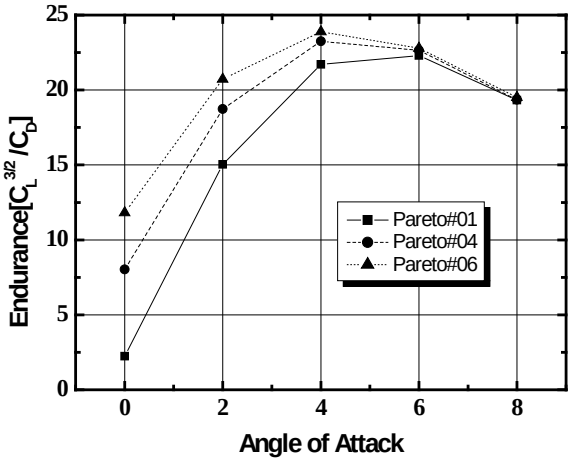

Fig. 6 Endurances vs. angle of attack for Pareto optima

airfoil at the root for the selected Pareto optima (solid lines) and base model (dotted lines) are presented in Fig. 7. It can be seen in Fig. 7(a) that the wing shape and the pressure distributions are almost same ones between the Pareto#01 and base model. The pressure contours of the Pareto#01 are, however, shifted to ahead compare with those of base model. This is resulted from the fact that both of them have the similar values of the lift and lift-to-drag ratio but the different value of the pitching moment as discussed in Fig. 4(c) and (d). For the case of Pareto#06 (Fig. 7(b)), the distributions of pressure are dramatically changed compare with the base model. Note that the Pareto#06 indicates one of the optimal solutions of the maximized the lift and lift-to-drag ratio and the minimized the pitching moment.

II. Conclusions

The shape optimization for airfoil of UAV which is required a high payload, economic operation, easy maneuver and high stability was performed numerically.

The design variables were parameterized by the Bezier curve and its number can be reduced by 11 owing to our previous study for two-dimensional situation. In addition, the sweep and taper ratio are added as the design variables because of the optimization of three- dimensional airfoil shape. The lift, lift-to-drag ratio and pitching moment are adopted as the objective functions for maximizing and/or minimizing the performance functions. For the optimization, the SMOGA which was developed by the author and the full Navier-Stokes solver were used, simultaneously.

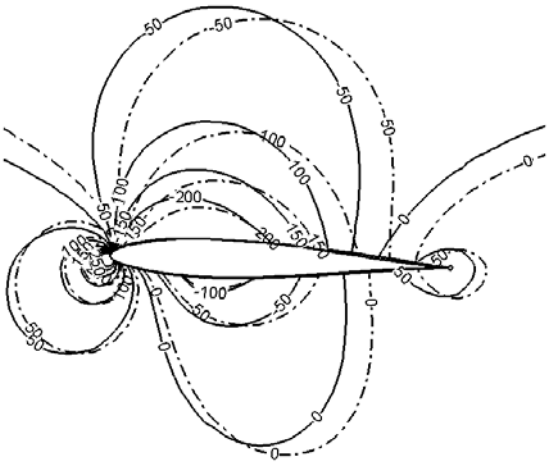

(a) (a) Pareto#01(solid line) and base model (dotted line)

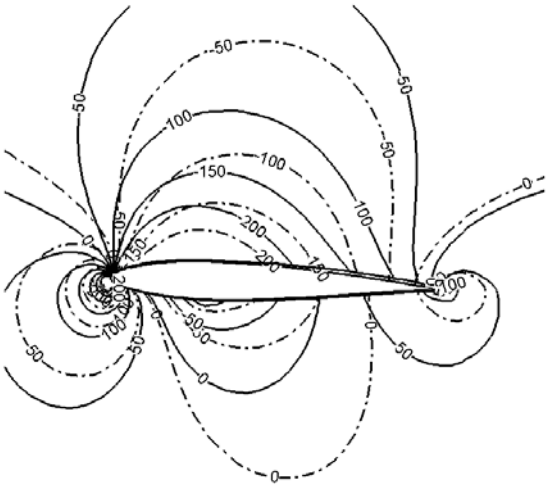

(b) Pareto#06 (solid line) and base model (dotted line)

Fig. 7 Pressure contours and shape of wing for selected Pareto optima and base model

The results showed that the rectangular shape without the sweep ($\omega = 0$ and $CR = 1$) for a high aspect ratio (AR = 17.5) was favored from the point of aerodynamic characteristics. The lift and lift-to-drag ratio did not show a clear trade-off in the given design space while the relationship between the pitching moment and other two objective functions had a sharp trade-offs. As the results of optimization, sixty-four non-dominated individuals (i.e., Pareto optima) could be obtained after twenty- five evolutions by exploring the entire design spaces and they will be the potential solutions for the long endurance UAVs. Thus, the UAV designer can select one of them according to the aerodynamic design target. The SMOGA constructed both for global and multi-objective optimization problems was able to manage for finding all

potential solutions in the given design environment.

Acknowledgment

This work was supported by the Korea Institute for Advencement of Technology(KIAT) grant funded by the Korean government(Motie : Ministry of Trade, Industry & Energy) 2017 (No. N0002431)

.

References

[1] H. C. Hwang and K.J. Yoon, "2004 International MAV Competition and Analysis for the MAV Technologies", *Journal of KSAS(Korean)*, 2004.

[2] S.A. Cambone, K.J. Krieg, P. Pace, and W. Linton, "Unmanned Aircraft Systems Roadmap 2005-2030," Office of the Secretary of Defense, 2005.

[3] D. Schawe, C.H. Rohardt, and G. Wichmann, "Aerodynamic design assessment of Strato 2C and its potential for unmanned high altitude airbone platforms," *Aerospace Science and Technology* No. 6, 2002, pp43-51.

[4] Z. Goraj, "Design challenges associated with development of a new generation UAV," *Aircraft Engineering and Aerospace Technology: An International Journal*, Vol. 77, No. 5, 2005, pp.361-368.

[5] T. G. Grabowski, A. Frydrychewicz, Z. Goraj and Suchodolski, "MALE UAV design of an increased reliability level," *Aircraft Engineering and Aerospace Technology: An international Journal*, Vol. 78, No. 3, 2006, pp 226-235.

[6] S. Painchaud-Ouellet, C. Tribues, J.Y. Trepanier, and D. Pelletier, "Airfoil Shape Optimization Using a Nonuniform Rational B-Splines Parametrization Under Thickness Constraint," *AIAA Journal*, Vol. 44, No. 10, 2006, pp. 2170-2178.

[7] D.J. Pines and F. Bohorquez,., "Challenges Facing Future Micro-Air- Vehicle Development," *Journal of Aircraft*, Vol. 43, No. 2, 2006, pp.290-305.

[8] T.T.H. Ng and G.S.B. Leng, "Application of genetic algorithms to conceptual design of a micro-air-vehicle," *Engineering Applications of Artificial Intelligence*, Vol 15, 2002, pp439-445.

[9] A.S. Fraser, "Simulation of genetic systems," *Journal of Theoretical Biology*, 1962, pp. 329–349.

[10] J.H. Holland, *Adaptation in Natural and Artificial Systems: an Introductory Analysis with Applications to Biology, Control, and Artificial Intelligence*, MIT Press, Cambridge, 1975.

[11] D. Goldberg, *Genetic Algorithms in Search, Optimization and Machine Learning*, Addision-Wesley, 1989.

[12] A.C. Poloni, A. Giurgevich, L. Onesti, and V. Pediroda, "Hybridization of a Multi-Objective Genetic Algorithm, a Neural Network and a Classical Optimizer for a Complex Design Problem in Fluid Dynamics", *Dipartimento di Energetica Universita di Trieste*, Italy, 1999.

[13] L.B. Booker, Improving Search in Genetic Algorithms," in Davis L (Editor), *Genetic Algorithms and Simulated Annealing*, Morgan Kaufmann Publishers, Los Altos, CA 1987.

[14] J. Lee, S. Lee, and K. Park, "Global Shape Optimization of Airfoil Using Multi-Objective Genetic Algorithm," *Transaction of KSME B*, Vol. 29. No. 10, 2005, pp. 1163-1171.

[15] STAR-CD v3.20 Methodology, Computational Dynamics, Co., London. U. K, 2004

[16] K.W. McAlister and R.K. Takahashi, "NACA0015 Wing Pressure and Trailing Vortex Measurements," NASA Technical Paper 3151, November 1991.

[17] K. Dejong, "An Analysis of the Behavior of a Class of Genetic Adaptive Systems," Doctoral Thesis, Department of Computer and Communication Sciences, University of Michigan, Ann Arbor, 1975

[18] J.D. Anderson, Jr, *Aircraft Performance and Design*, McGraw-Hill, 1999, Chap 2.

Byeong Sam, Kim Prof. Byeong Sam Kim is currently working at Department of Mechanical Engineering in Hoseo University as a professor. he acquired his Ph.D. degree in 1995 at Ecole Polytehnique, Paris, France, he entered the GM DAEWOO Technical center., and he researched on CAE team for crashworthiness. In 1998, he joined the Laboratory composite process at Ecole Polytenique Federale de Lausanne(EPFL) for two and half years, and studied about polymers processing with FEM. His main interesting fields are computer aided engineering, inelastic structures, an optimization. Recently, his researches are focus on the semiconductor and display manufacturing process and crashworthiness vehicles.

Byung Ryoun Kim PhD candidate Byung Ryoun Kim is currently working at Department of Mechanical Engineering in Hoseo University.

Chakun Cheong Prof. Chakun Cheong is currently working at Department of Mechnical Engineering in Hoseo University as a professor. he acquired his Ph.D. degree in 1994 at Toyko University, Toyko, Japan, he entered the LG Electronics., and he researched on control system and telecommunication.

Kyoungwoo Park Dr. Kyoungwoo Park is currently working at Department of Mechanical Engineering in Hoseo University as a professor. He has received his BA degree in 1985, MA degree in 1990, and Ph.D. degree in 1995, respectively, at the department of mechanical engineering of Hanyang University, Seoul, Korea. As soon as he acquired his Ph.D. degree, he joined to the LG Industrial Systems Co., Ltd., and he researched on the flow and thermal characteristics around/in elevators. In 1999, he joined the Ralph Greif research team for two and half years, who is a professor of University of California at Berkeley and studied about convection heat transfer with CFD. After he came back to Korea in 2001, he researched and taught students at IDOT of Hanyang University until Feb. 2005. His main interesting fields are heat transfer, micro/macro thermo/fluid dynamics, optimization, and CFD. Recently, his researches are focus on the semiconductor and display manufacturing process and the aerodynamics and optimization of thermo/fluidics system.